# Adaptive Protection and Control in the Power System for Wide-Area Blackout Prevention

M. A. M. Ariff, *Member, IEEE*, and B. C. Pal, *Fellow, IEEE*

***Abstract*—This paper presents a new approach in adaptive out-of-step (OOS) protection settings in power systems in real time. The proposed method uses extended equal area criterion (EEAC) to determine the critical clearing time and critical clearing angle of the system, which are vital information for the OOS protection setting calculation. The dynamic model parameters and the coherency groups of the system for EEAC analysis are determined in real time to ensure that the newly calculated settings suit with the prevalent system operating condition. The effectiveness of the method is demonstrated in simulated data from a 16-machine 68-bus system model.**

***Index Terms*—Adaptive protection, coherency identification, dynamic model parameter estimation, measurement based, out-of-step (OOS) protection , phasor measurement unit (PMU), synchrophasors.**

## I. Introduction

CONVENTIONAL power system protection relays operate on the basis of settings. Anatomy of several blackouts revealed that the relays with such settings at times mal-operate under very stressed operating conditions [1]. This is because of the fact that the electrical characteristics exhibited by the system in some stressed operating conditions are not captured during relay settings calculation process, both in the factory and the field. An extensive report by IEEE Power and Energy Society (PES) corroborated this fact [1]. One vital recommendation from this report is to adapt the protection setting to suit to the prevalent system operating situation.

Recent efforts on adaptive OOS protection systems have been reported in the literature [2]–[5] and [6]. The work in [2] has reported an adaptive OOS relay based on neural network method. The technique provides a satisfactory performance in detecting OOS condition and provides appropriate control action following the disturbance, provided that the neural network had been trained to deal will all possible contingencies. Researchers in [3] reported an adaptive OOS technique based on equal-area criterion (EAC) method. However, the technique assumed that coherent group of generators would not change following a severe disturbance in the system, which may not always be the case in practice. The adaptive OOS relay schemes reported in [4] applied the EAC in time-domain to the OOS detection problem. However, the utilisation of EAC method is limited only to the application on single machine infinite bus system (SMIB) [7]. The work in [6] discussed the detection of OOS condition using frequency deviation of voltage. Similar to the work reported in [4], the derivation of the method reported in the paper is based on EAC method. Therefore, it is also limited only to the application on SMIB. This limitation also applies to the method reported in [5] that has used state-plane trajectory analysis to detect OOS condition. Although the concept of adaptive relaying offers substantial rewards in improving the security and integrity in network operation, protection engineers have some sense of nervousness to implement the concept of adaptive relaying in practice [8]. This sense of nervousness comes from the requirement of ignorance of the protection settings if any of the methods reported in [2]–[5] and [6] is implemented in practice. All of these methods directly assess the system stability from the measured data following a disturbance in the system instead of using protection settings to detect OOS condition. In contrast, the method proposed in this paper adapts the settings of conventional OOS relay to suit the prevalent system operating condition. So the work presented in this paper provides an option that strikes a balance between the existing practice in industry and usefulness of the adaptive relaying philosophy. The proposed method does not require any prior information of the system as the proposed algorithm estimates the time critical dynamic properties of the system that influences the settings of an OOS relay.

The idea presented in this paper is inspired from the results reported in [9] and [10]. The adaptive protection schemes in [9] and [10] determine several groups of settings based on criteria that influence the sensitivity of protection scheme. The work in [9] determines the groups of settings based on the level of biasness towards security or dependability of relay operations. On the other hand, the work reported in [10] determines the groups of settings based on the zone reach of relay operation. Consequently, in both methods, a group of settings are selected from these groups based on the current operating conditions. The groups of relay settings are determined using the off line methods based on various heuristic assumptions of the system operating conditions. Even with the increased number of settings that suits with a number of system operating conditions, the relay may mal-operate if the unusual and stressed system

Manuscript received July 01, 2015; revised October 01, 2015 and December 11, 2015; accepted January 12, 2016. Date of publication February 03, 2016; date of current version July 21, 2016. This work was supported in part by EPSRC, U.K.under Grants ACCEPT and EP/K036173/1. Paper no. TPWRD-00848-2015.

M. A. M. Ariff is with the Faculty of Electrical and Electronic Engineering, Universiti Tun Hussein Onn Malaysia, 86400 Batu Pahat Johor, Malaysia (e-mail: mohdaifaa.mohdariff.1987@ieee.org).

B. C. Pal is with the Department of Electrical and Electronics Engineering, Imperial College London, London SW7 2AZ, U.K. (e-mail: b.pal@imperial.ac.uk).

Color versions of one or more of the figures in this paper are available online at http://ieeexplore.ieee.org.

Digital Object Identifier 10.1109/TPWRD.2016.2518080

operating condition is not anticipated during the off-line determination of groups of relay settings. The work presented in this paper proposed an useful adaptive OOS protection scheme that calculates the settings of the relay online, based on the timely estimations of the dynamic characteristics of the system. Next section discusses the settings for blinder scheme used in OOS protection.

## II. Out-of-Step Protection Scheme

With time power networks evolve; additional transmission lines are built, new generators are added and the demands grow. Such evolution significantly changes the electrical characteristics (impedance locus) of the system such as, the ratio between the generator impedance and the network system impedance. With addition of transmission circuits, the system impedance centre and electrical centre tend to occur within the generator or its corresponding step-up transformer rather than within the transmission network following a power swing in the system. Such situation causes abnormally high stator core end iron fluxes in the generator which consequently lead to overheating and short circuits at the stator core ends. Therefore, it is necessary to have an OOS relay that will detect and initiate appropriate control action to avoid these adverse effects on the affected generator and the rest of the system.

There are a number of options to protect a generator against OOS condition. These methods are diverse such as the single-blinder, double blinder, and concentric schemes [11]. Basically, all these schemes operate on the same principle, that is monitoring the behaviour of the impedance swing following a disturbance in the system. It is necessary to perform an extensive transient stability study to determine the appropriate setting for an OOS protection scheme. However, in the absence of results from transient stability studies, the setting of an OOS protection scheme may be determined using a graphical procedure and conservative settings. This paper focuses on adapting the setting of single blinder scheme for effective matching with the prevailing operating conditions as it is easy to implement in a numerical relay [11]. Fig. 1 depicts the impedance setting of a single blinder setting for generator OOS protection. The figure suggests the calculation of the setting of the OOS relay requires several important parameters of the generator and the system such as generator transient reactance $x'_d$, unit transformer reactance $X_{TR}$, and system impedance $Z_{SYS}$. The supervisory mho element is set to reach 1.5 times the unit transformer impedance in the system direction and two times the generator transient reactance in the generator direction. The diameter $D_{mho}$ and the centre $C_{mho}$ of the mho characteristic are calculated as follows [12]:

$$D_{mho} = 2 \times x'_d + 1.5 \times X_{TR} \tag{1}$$

$$C_{mho} = 1.5 \times X_{TR} - \frac{D_{mho}}{2} \tag{2}$$

It is essential to determine the CCA $\delta_{CRIT}$ between the generator and the system in order to calculate the setting of the relay. The CCA occurs at the point when the generator begins to lose its synchronism with the system. This angle is obtained from transient stability studies of the system. General practice within the industry uses 120° angle because usually the system is not

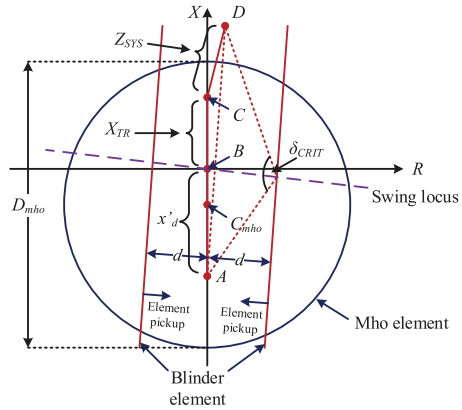


Fig. 1. Procedure to set OOS relays.

able to recover from the swing at this angle. Consequently, the setting of the blinder is calculated using the following equation [12]:

$$d = \frac{x'_d + X_{TR} + Z_{SYS}}{2} \times \tan\left(120^\circ - \frac{\delta_{CRIT}}{2}\right) \tag{3}$$

The next step is to determine the time for the impedance swing to travel between the blinder elements. In order to implement the scheme that requires a minimum traverse time between the blinders, the time delay should be set to a value corresponding to the fastest travel time between the two blinders. Setting the timer delay too short may jeopardize the sensitivity of the relay. An appropriate time delay is crucial to prevent relay maloperation during transient event in power system operation.

## III. Adaptive Out-of-Step Protection Algorithm

The calculation of an OOS relay setting is straightforward when the CCA, CCT, and generator dynamic parameters are known. The procedure to approximate the CCA and CCT to determine the setting of OOS protection is the most exhaustive part of the process. In this paper, the computational effort required is simplified by using the EEAC approach described in [13]. The implementation of EEAC involves the transformation of a multi-machine system into a two-machine system. Then two-machine system is further simplified into a single-machine infinite bus system.

With the SMIB system equivalent, a standard EAC is used for stability analysis to determine the CCA and CCT of the system, which is crucial step to calculate the settings of OOS protection. However, to ensure the relay setting is adapting to the current operating condition, the real-time information of the coherent groups of generators and the dynamic model parameters in the system are required to analyse a large interconnected network using EEAC. The method reported in [14] facilitates an elegant solution to identify the coherent group of generators in the system. On the other hand, the dynamic model parameters estimation technique elaborated in [15] are able to estimate these parameters in real-time.

Fig. 2 shows the algorithms of the proposed method to recalculate and retune the setting of an out-of step protection system. An algorithm performing such functions automatically for an OOS protection system requires several input measurements, a

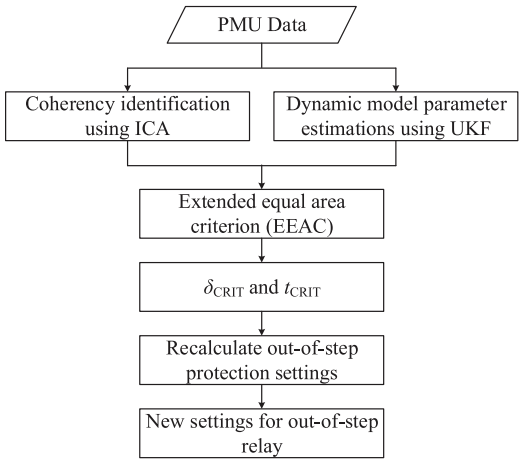


Fig. 2. The algorithm for adaptive OOS protection scheme.

current equivalent power system model and protection system constraints to perform the calculation. The proposed algorithm displayed in the figure is initiated by a change in power system condition that is monitored from the oscillation in the measured data. Since the OOS event is classified as a wide-area stability problem [7], measurements across a wide geographical area will be required for a large power system network. WAMS technology is able to facilitate the measurements required. The measured data obtained from the WAMS is gathered at a single supervisory control centre for analysis. The measurement of voltage magnitude, angle, active and reactive power, from the grid supply points and the large generations in the system are required for the algorithm. The accuracy of the measurement considered in this study is as recommended by the recent IEEE standard for Synchronization, Calibration, Testing, and Installation of Phasor Measurement Units (PMUs) for Power System Protection and Control C37.242-2013 [16]. It is recommended that the measurement have the time tagging with accuracy better than 1 $\mu$s and the magnitude with accuracy of 0.1% [16]. In the control centre, the coherent groups of generators are identified using the method proposed in [14] and the dynamic model parameters of the generators in the system are estimated using the method proposed in [15]. The identified coherent groups and the estimated dynamic model parameters of generators represent the temporal dynamic properties of the system. The EEAC method is then used to determine the CCA and CCT of the system. This is realised by using an equivalent power systems model constructed using the timely dynamic properties obtained in the previous step. Subsequently the OOS relay settings are calculated using the value of CCA and CCT obtained from the EEAC method.

The accuracy of the CCA and CCT estimations are vital to the performance of the proposed algorithm in adapting the OOS relay settings. The estimation of CCA and CCT are important in determining the time required for the impedance trajectory to traverse across the blinder settings [17]. Therefore, an inaccurate estimation of CCA and CCT may cause relay to mal-operate, consequently causing a negative impact on the system stability. In the literature, many algorithms have been proposed to estimate CCA and CCT of the system [18]–[22]. However, there is no report on actual implementation of these methods. In the proposed algorithm, the CCA and CCT are estimated using EEAC method [13]. The consideration of EEAC is based on the study reported in [23]. The report reviews the state of the art in online transient stability assessment. The study conducts a literature survey from vendors who have fully developed and market the online transient stability assessment tools. The report concluded that 4 out of 6 vendors utilised the EEAC method in their online transient stability assessment tools and these tools have been widely used in practice, particularly for protection relay commissioning [8]. This implies that the EEAC method provides satisfactory performance and accuracy to be applied in practice.

### A. Coherency Identification Using ICA

This section provides a brief discussion on the coherency identification using ICA as reported in [14]. From the report, spectral ICA is applied to the voltage angle of generator bus following a disturbance in the system. Each voltage angle of generator bus is represented by a row vector of data matrix. The row vectors of data matrix for the spectral ICA model, are single sided power spectra of mean centred time trends over a range of frequency, up to the Nyquist frequency:

$$\boldsymbol{X}(\boldsymbol{f}) = \begin{pmatrix} P_1(f_1) & \cdots & P_1(f_N) \\ \vdots & \ddots & \vdots \\ P_m(f_1) & \cdots & P_m(f_N) \end{pmatrix} \tag{4}$$

The power spectrum can be obtained using Discrete Fourier Transform (DFT) to the mean centred time trend. Then, each power spectrum is normalised. Each vector in $\boldsymbol{X}$ is a linear mixture of hidden and independent process. Each process forms a row vector in $\boldsymbol{S}$. Each row in $\boldsymbol{S}$ is an IC. These processes are represented by an ICA mixing model given by:

$$\boldsymbol{X}(\boldsymbol{f}) = \boldsymbol{A}_{m\times n} \begin{bmatrix} s_1 \\ s_2 \\ \vdots \\ s_n \end{bmatrix} = \boldsymbol{A}_{m\times n}\boldsymbol{S} \tag{5}$$

where, $\boldsymbol{A}$ is an unknown $m \times n$ matrix of full rank, called the *mixing matrix*. The main aim of ICA is then to estimate $\boldsymbol{S}$ and the mixing matrix, $\boldsymbol{A}$ from the observed normalised power spectrum, $\boldsymbol{X}$. This is realised by using the fast fixed-point algorithm reported in [24]. This algorithm uses a very simple yet highly efficient fixed point iteration technique.

However, the sign, the magnitude and the order of ICs obtained are not unique. So, additional constraints are imposed on the ICA mixing model for physically meaningful results. All ICs are adjusted to have positive peak values to enhance visualisation. The mixing matrix is also scaled so that relationships between the spectral signatures and ICs are easily identified. The order of ICs is also sorted in order to properly visualise the coherency property of the system. Following these processes, the ICA decomposition in (4) is rewritten as follows:

$$\boldsymbol{X}(\boldsymbol{f}) = \begin{pmatrix} \boldsymbol{t}_{1,1} \\ \vdots \\ \boldsymbol{t}_{i,1} \end{pmatrix} \boldsymbol{c}_1' + \begin{pmatrix} \boldsymbol{t}_{1,2} \\ \vdots \\ \boldsymbol{t}_{i,2} \end{pmatrix} \boldsymbol{c}_2' + \begin{pmatrix} \boldsymbol{t}_{1,3} \\ \vdots \\ \boldsymbol{t}_{i,3} \end{pmatrix} \boldsymbol{c}_3' + \boldsymbol{E} \tag{6}$$

where

$$\boldsymbol{E} = \begin{pmatrix} \boldsymbol{t}_{1,4} \\ \vdots \\ \boldsymbol{t}_{i,4} \end{pmatrix} \boldsymbol{c}'_4 + \cdots \begin{pmatrix} \boldsymbol{t}_{1,n} \\ \vdots \\ \boldsymbol{t}_{i,n} \end{pmatrix} \boldsymbol{c}'_n$$

The first part in (6) involving $c'_1, c'_2$ and $c'_3$ represents three most dominant ICs. The last part, $\boldsymbol{E}$ represents the rest of the process. The three-tuple ($t_{i,1}, t_{i,2}$ and $t_{i,3}$) is a point in three-dimensional dominant IC space. The IC space has the advantage of displaying coherent groups as tightly formed clusters. All three-tuples from different rows of $\boldsymbol{T}$ are plotted in the IC space. The three-tuples that are close to each other in the IC space represent coherent signals. Since each row signifies a signal from a generator or bus, all generators or buses captured in the cluster form coherent groups. This formation of clusters is used to identify coherent areas in the system. The method reported in [14] provides an analytical tools for coherency identification in power system based on WAMS.

### *B. Dynamic Model Parameter Estimation Using UKF*

This section presents the dynamic model parameter estimation using UKF. This technique estimates the parameters that influence the performance of OOS relay. From [15], the power system first swing dynamics are represented as follows:

$$\frac{d\delta(t)}{dt} = (\omega(t) - \omega_0)\omega_s \tag{7a}$$

$$\frac{d\omega(t)}{dt} = \frac{1}{2H}\left(P_m - P_g(t) - D(\omega(t) - \omega_0)\right) \tag{7b}$$

where $\delta(t), \omega(t), \omega_0$ and $\omega_s$ are rotor angle, rotor speed, synchronous speed and base speed, respectively. This study focuses on the estimation of parameters that influence settings of an OOS protection. These settings are mainly influenced by $E_q, x'_d$ and $H$. Neglecting the damping coefficient $D$, the discrete form of (7) is given by:

$$\delta_k = \delta_{k-1} + (\omega_{k-1} - \omega_0)\omega_s \triangle t \tag{8a}$$

$$\begin{aligned} \omega_k &= \omega_{k-1} + \frac{\triangle t}{2H_{k-1}}\left(P_m - P_{g_{k-1}}\right) \\ &= \omega_{k-1} + G_{k-1}\left(P_m - P_{g_{k-1}}\right) \end{aligned} \tag{8b}$$

Since $\triangle t$ and $H_k$ are constant, $\omega_k$ is simplified by substituting the term $\frac{\triangle t}{2H_k}$ with $G_k$ to reduce the nonlinearity of the equation. Consequently, the state vector of the system is defined as $\boldsymbol{x}_k = \begin{bmatrix}\delta_k & \omega_k\end{bmatrix}^\top$ and is parameterized by inertia constant $H$, transient impedance $x'_d$ and generator internal voltage $E_q$. These parameters and variable are unknown and represented by the vector $\boldsymbol{\psi}_k = \begin{bmatrix}E_{q_k} & x'_{d_k} & G_k\end{bmatrix}^\top$. The state $\boldsymbol{x}_k$ and the unknown parameter vector $\psi_k$ are simultaneously estimated by augmenting these two vectors into a higher-dimensional state variables $\boldsymbol{x}^a_k = \begin{bmatrix}\delta_k & \omega_k & E_{q_k} & x'_{d_k} & G_k\end{bmatrix}^\top$. Therefore, the state evolution equation in (8) is reformulated as:

$$\delta_k = \delta_{k-1} + (\omega_{k-1} - \omega_0)\,\omega_s \triangle t \tag{9a}$$

$$\omega_k = \omega_{k-1} + G_{k-1}\left(P_m - P_{g_{k-1}}\right) \tag{9b}$$

$$E_{q_k} = E_{q_{k-1}} \tag{9c}$$

$$x'_{d_k} = x'_{d_{k-1}} \tag{9d}$$

$$G_k = G_{k-1} \tag{9e}$$

In (9), the mechanical input power $P_m$ is assumed to be known. It is assumed that PMU provides time-tagged voltage magnitude $V_g$, phasor angle $\theta_g$, active power $P_g$ and reactive power $Q_g$ measurements for the algorithm. $V_g$ and $P_g$ are treated as the input signals, while $\theta_g$ and $Q_g$ are treated as the measurements to decouple one generation unit from the rest of the system. The equations for the measurement quantities, $\theta_g$ and $Q_g$ of a generation unit are:

$$\theta_{g_k} = \delta_k - \tan^{-1}\left(\frac{P_{g_k} x'_{dk}}{\sqrt{\left(E_{q_k} V_{g_k}\right)^2 - \left(P_{g_k} x'_{dk}\right)^2}}\right) \tag{10a}$$

$$Q_{g_k} = \frac{\sqrt{\left(E_{q_k} V_{g_k}\right)^2 - \left(P_{g_k} x'_{dk}\right)^2} - {V_{g_k}}^2}{x'_{dk}} \tag{10b}$$

The UKF algorithm as described in [25] will be directly applied to estimate $\boldsymbol{x}^a_k$. The estimation of $\boldsymbol{x}^a_k$ provides the estimation of the unknown parameters of inertia constant $H$, transient impedance $x'_d$ and generator internal voltage $E_q$. The dynamic model parameters estimation using UKF [15] is able to estimate the dynamic model parameters of the system that influence the settings of OOS relay accurately without prior information of the test system model. The maximum error of the estimated parameters for the application on the 16-machine 68-bus test system model is equal to 3.26% [15].

## IV. Timeline for OOS Settings Adaptation

The proposed algorithm requires the knowledge of the coherent groups and the dynamic model parameters of the generators in the system. These are obtained using the methods proposed and demonstrated in [14] and [15], respectively. The methods proposed in [14] and [15] require information from the oscillation in the measured data, which can be observed during the change in the system operating condition. Therefore, the execution of the proposed algorithm starts when there is an oscillation in the measured data representing the change in the system operating condition.

The proposed coherency identification technique requires a data time windows 5.0 s of measurements to monitor the coherency properties of the system effectively [26]. The requirement of the data time windows for coherency identification technique depends on the nature of the electromechanical oscillation of the system. The data time windows of 5.0 s allow the detection of mono-frequency signals with the frequency down to 0.2 Hz. These signals represent the inter-area oscillation of the system [27]. Shortening the data-time windows may result to the failure in detecting the inter-area oscillations in the system; consequently affect the accuracy of any data-driven coherency identification method. In this paper, continuous identification of coherent group of generators using ICA with 5.0 s moving data time windows is considered in the proposed algorithm. Using this approach, the ICA method is able to identify the coherent group of generators after 2.0 s after the start of oscillation if ambient conditions is considered prior to the disturbance. In practice, the measured signals are influenced not only by the transmission system itself but also the random load fluctuations that continuously deviate the system equilibrium slightly but also in a nonstationary manner. This is an advantage of the application

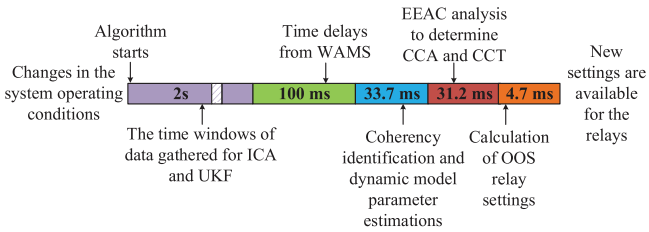


Fig. 3. The time-line for adaptive OOS relay operations.

of ICA method because it is able to estimate the electromechanical oscillation under ambient condition [28]. The proposed dynamic model parameter estimations technique requires a time windows of approximately 1.0 s to be able to estimate the parameters accurately. In addition, the required measured data is gathered at a centralised supervisory control centre from PMU located at grid supply points or large generators via various level of PDC hierarchy. This process also introduces a time delay in the order of 30–100 ms [29].

Fig. 3 shows the time-line of the operation of the algorithm operation for adaptive OOS protection proposed in this paper. From the figure, the proposed method is able to provide new settings to an OOS relay following a change in the system in approximately 2.2 s after the start of oscillation. Also, it is noted that the time required for the proposed algorithm to calculate the new settings is within the time-frame of first swing stability. However, the computation time for the proposed algorithm alone as recorded in MATLAB Simulink environment using Intel Xeon L5520 2.26 GHz quad-core processor with 12 GB DDR3 RAM platform is $33.6 + 31.2 + 4.7 = 69.6$ ms. This implies that the method proposed for adaptive OOS protection system computes new settings for an OOS relays within 4 cycles of power frequency from the moment the data is available at the centralised control centre. An additional amount of time is required to retune the OOS settings for a larger test system. However, the additional time required is relatively insignificant because most of the time required to adapt the OOS settings are utilised for data gathering using WAMS. The settings are updated in the relay logic to protect the system from an OOS condition. The fundamental of OOS relay is based on the principle of distance relay. Therefore, there are always coordination requirement with the time discrimination of zonal protections of distance relay, especially during the load encroachment and delayed back up protection [30]. Fortunately the variation of fault impedance seen with time is very distinct for power swing cases. So co-ordination is not difficult but requires systematic approach involving distance protection elements. The scope of this study is limited to the calculation of OOS settings only. This will be pursued in the immediate future research.

## V. Determination of OOS Protection Settings

The 16-machine 68-bus test system model is considered in this investigation. The bus data, line data and dynamic characteristics of the systems are available in [31], [32]. A nonlinear simulations of the test system model are performed in MATLAB Simulink. The synchronous generators are represented through classical models. The mechanical power inputs to the generators

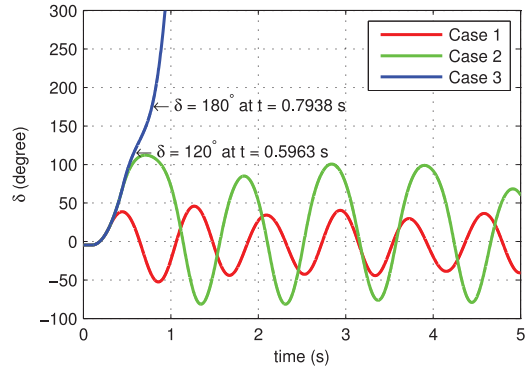


Fig. 4. Rotor angle for Generator #10 for all three cases.

TABLE I
Pre-Determined OOS Relay Settings

| Setting | Value of setting |
|---|---|
| $d$ (pu) | 0.0244 |
| $D_{mho}$ (pu) | 0.1201 |
| $C_{mho}$ (pu) | -0.0211 |
| Time to cross both blinders (ms) | 396 |

are assumed to be constant. This study demonstrates the procedure to determine the setting of the mho element, the blinder and the time delay for the impedance swing to cross both blinders for generator OOS protection. A three phase temporary fault at Bus #31 is considered as disturbance in this study. For demonstration purposes, this section focuses on the settings determination and performance evaluation of OOS relay for Generator #10. The settings for OOS relay for other generators in the system can be calculated in the similar manner. The study starts with a fault clearing time of 200 ms with iterative increments of 10 ms until the generator is going OOS from the rest of the system. The fault clearing time considered for each representative case are listed as follows:

1) Case 1—Fault cleared after 200 ms
2) Case 2—Fault cleared after 330 ms
3) Case 3—Fault cleared after 340 ms

Fig. 4 displays the rotor angle for Generator #10 for all representative cases considered, each with a different fault clearing time. From the figure, it is observed that Generator #10 remains in synchronism when the fault is cleared 200 ms following the fault initiation at Bus #31. In Case 2, the generator still remains in synchronism with the system with a fault clearing time of 330 ms. However, the system loses it synchronism when the fault is cleared 340 ms after the fault inception in the system. This implies that the CCT for the generator to remain in synchronism with the system is approximated equal to 330 ms. Also, it is observed from the figure that the CCA is approximately 120° at time of 596 ms. The approximated CCA is used to determine the setting of the blinder element using (3). The time for the swing impedance locus to travel from the CCA to 180° is approximately 198 ms. Therefore, the travelling time within the blinder should be set at 198 ms $\times$ 2 $=$ 396 ms. The setting of the supervisory mho element is calculated using (1). Table I summarises the pre-determined settings used in this

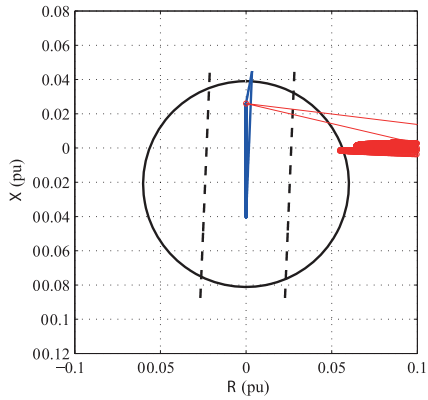


(a)

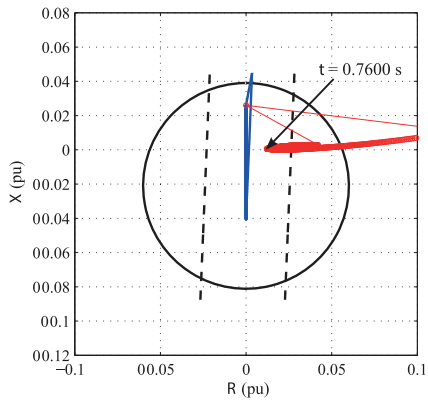


(b)

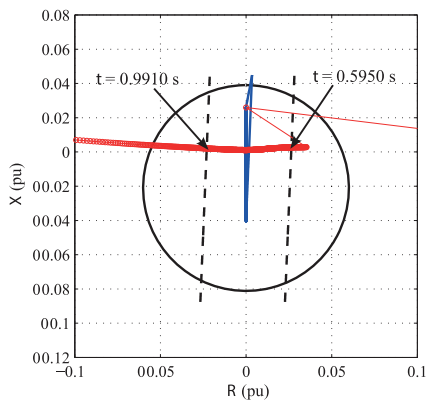


(c)

Fig. 5. Impedance trajectories for (a) Case 1 (b) Case 2 (c) Case 3.

paper. Fig. 5 shows the OOS protection setting for Generator #10 and the swing impedance trajectory for all three cases. In the figure, the red, blue, and black lines represent the swing impedance seen by the relay, the line impedance covered by the relay and the settings of the relay (supervisory mho and blinder elements), respectively. From Fig. 5(a), it is observed that the swing impedance encroaches the supervisory mho elements. However, the swing impedance does not cross any blinder element of the relay. Therefore, the OOS relay will not trip the generator under this condition because it does not cross the blinder element of the relay as it is a stable swing. Fig. 5(b) shows the swing impedance for Case 2. The figure shows that the swing impedance penetrated the supervisory mho element and crossed the blinder on the right-hand side of the figure, and consequently starts the timer for the blinder elements of the relay. However, the swing impedance goes to the opposite direction after $t = 760$ ms, hence does not cross the blinder on the left-hand side of the figure. Therefore, the OOS relay does not recognize this condition as an OOS condition. Fig. 5(b) demonstrates that the swing impedance crosses the relay blinder element at $t$ equals to 595 ms and consequently crosses the other blinder element at $t$ equals to 994 ms. Therefore, the travelling time for the swing impedance to cross the relay element is equals to 399 ms which exceeds the time delay setting of the relay. Consequently, the relay recognized this event as an OOS condition and issues tripping signal to isolate the generator from the system. It is clear that from the first two cases, the impedance trajectory does not cross the line of impedance of the system whereas the swing impedance crosses both blinder elements in the third case. Therefore, the relay only recognized the third case as an OOS condition. The outcome of the OOS protection decision is consistent with the rotor angle responses illustrated in Fig. 4. It is shown that the sensitivity and reach of the generator OOS relays are influenced by the dynamic model parameters seen by the relay sensor. The generator OOS relay setting determined in this section operates in a fixed manner. Therefore, changes in these parameters may cause the OOS relay to mal or mis operates and further exacerbates the impact of disturbance in the system. Adapting the OOS protection setting according to these changes improves the reliability and security of the relay operation.

The proposed method calculates the OOS relay setting using the up-to-date information of dynamic signature of the system. The measured data gathered via WAMS are analysed using ICA [14] and UKF [15] to determine the coherent group of generators and the dynamic model parameters of the system, respectively. Consequently, EEAC is utilised to estimate the CCA and CCT using the up-to-date dynamic properties of the system. The algorithm calculates the OOS relay settings based on the estimated CCA and CCT. The supervisory mho and the blinder settings are calculated using the equations given in (1) to (3) [11]. The time allowed to cross both blinders is set to the time of impedance traverse from one blinder to another under CCT operating condition [11]. Subsequently, the settings of OOS relays are updated with the newly calculated supervisory mho, blinders and traverse time across the blinders settings based on up-to-date system dynamic behaviour.

## VI. Performance Evaluation

In practice, the values of the generator dynamic model parameters will differ with time from the values supplied by the manufacturer. Inaccurate representation of dynamic model parameters is likely to have a significant impact on the system dynamic and frequency stability [1]. Furthermore, in the case of applying a relay for OOS protection for multiple units, the relay settings need to be updated regularly. This is due to the combined impedances and inertia constant seen by the relay depending on the number of generator being on-line and the network strength at that particular time [33]. The results of the three representative cases, namely Case A, B and C, each with different system

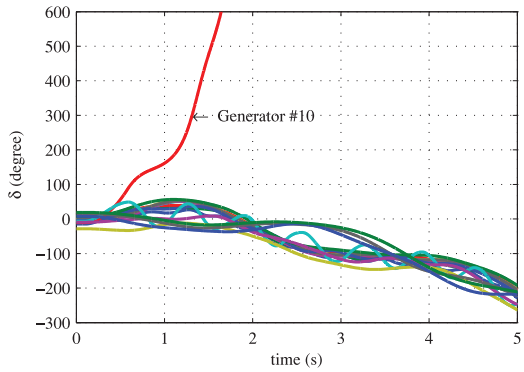


Fig. 6. Rotor angle for all generator for Case A.

operating conditions are presented and analysed. In this study, it is assumed that the total number of generator units in Generator #10 site is equal to three. During normal operating condition, only two out of three generators are connected to the system. Here, the changes in the generator operating condition is set arbitrarily only to demonstrate the influence of the generator dynamic parameters to the OOS relay operation. A three phase temporary fault at Bus #31 is considered as disturbance for this investigation. In order to study the generator behaviour under OOS conditions, for each case, the fault clearing time is chosen such that the generator will lose its synchronism with the rest of the system.

### A. Case A

In Case A, a three phase fault cleared 450 ms after the fault inception is considered as the disturbance in the system. It is assumed that all three generators are online which are represented by the 50% increase of the inertia constant and the 50% reduction of combined transient reactance in Generator #10 seen by the relay. Fig. 6 displays the rotor angle for all generators in the system for this case following the disturbance. The figure shows that the Generator #10 loses its synchronism with the rest of the system following the fault at Bus #31. In this condition, it is necessary to isolate the generator from the system to prevent severe damage to the affected generator shaft. Fig. 7 depicts the swing impedance trajectory on two different OOS protection settings. The setting illustrated in Fig. 7(a) represents the setting calculated based on the dynamic model parameters of Generator #10 operating at normal operation. In Fig. 7(b), the setting of the OOS relay is recalculated using the adaptive OOS protection scheme described in Fig. 2. The minimum time required for the swing impedance to cross both blinders for the pre-determined OOS relay setting and the adaptive OOS relay setting are 396 ms and 437 ms, respectively. Table II summarises the pre-determined settings and the adaptive settings of the OOS relay used for in Case A. The result shows that the swing impedance stays within both blinder elements of pre-determined relay setting in 639 ms while the swing impedance shown in Fig. 7(b) stays within the blinder elements of the adaptive relay setting in 528 ms. The time for the swing impedance to traverse both blinders exceeds the time delay setting for both relays. This implies that, both OOS relay settings are able to recognize the OOS condition in the system in this operating condition.

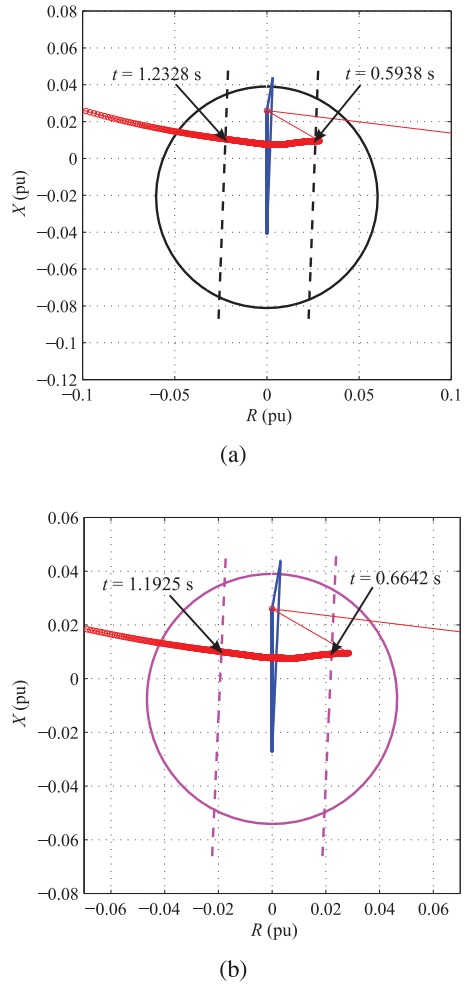


Fig. 7. Relay settings for Case A (a) Pre-determined (b) Adaptive.

TABLE II
OOS RELAY SETTINGS FOR CASE A

| Types of setting | Pre-determined | Adaptive |
|---|---|---|
| $d$ (pu) | 0.0244 | 0.0205 |
| $D_{mho}$ (pu) | 0.1201 | 0.0931 |
| $C_{mho}$ (pu) | -0.0211 | -0.0075 |
| Time to cross both blinders (ms) | 396 | 437 |

### B. Case B

A three phase fault cleared at 190 ms after the fault inception is considered as the disturbance in the system in Case B. In this case, it is assumed only one out of three generators is online. Therefore, there is a 50% decrease of the inertia constant and a 50% increase of the combined transient reactance in Generator #10 seen by the OOS relay element. Fig. 8 exhibits the generator rotor angle in the system following the disturbance considered for this case. The figure demonstrates that Generator #10 loses its synchronism during the first swing following the disturbance in the system. It is vital to separate the generator from the system to avoid severe damage to the generator and the system. Fig. 9 represents the swing impedance trajectory on two different relay settings. The OOS protection setting in Fig. 9(a) signifies the pre-determined OOS relay settings calcu-

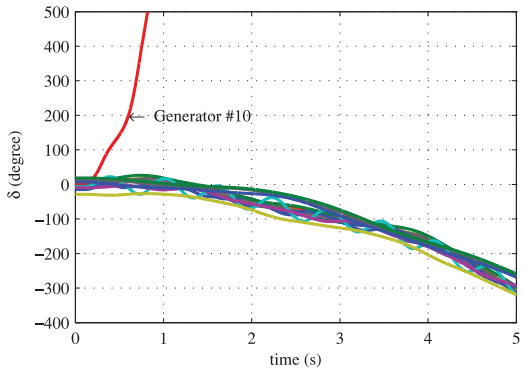


Fig. 8. Rotor angle for all generator for Case B.

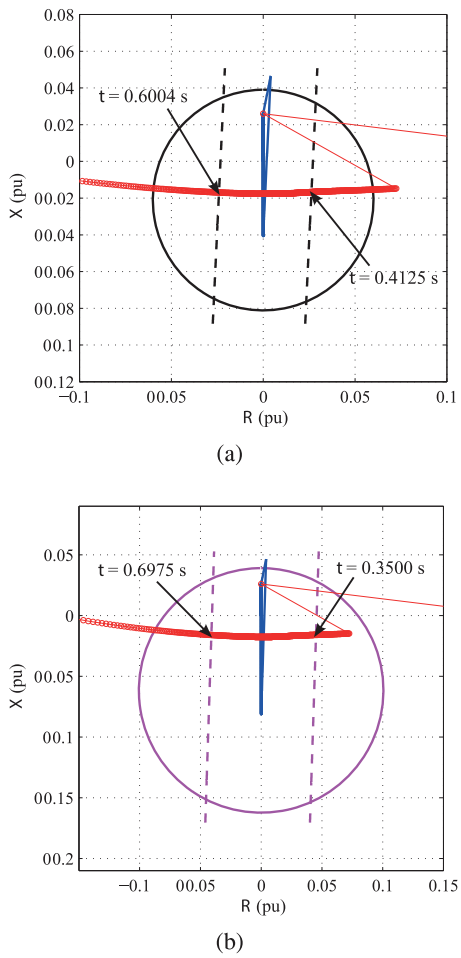


Fig. 9. Relay settings for Case B (a) Pre-determined (b) Adaptive.

lated based on the dynamic model parameters of Generator #10 operating at normal operating condition. In contrast, the settings of the adaptive OOS relay displayed in Fig. 9(b) are calculated using the approach elaborated in Fig. 2. The minimum time required for the swing impedance to cross both blinders in sequel for the pre-determined relay setting and the adaptive relay setting are 396 ms and 326 ms, respectively. Table III summarises the pre-determined settings and the adaptive settings of the OOS relay used for in Case B. It is observed from Fig. 9(a) that the swing impedance crosses both blinder elements in sequel of relay setting in 188 ms. This indicates that the time for the swing

TABLE III
OOS RELAY SETTINGS FOR CASE B

| Types of setting | Pre-determined | Adaptive |
|---|---|---|
| $d$ (pu) | 0.0244 | 0.0430 |
| $D_{mho}$ (pu) | 0.1201 | 0.2031 |
| $C_{mho}$ (pu) | -0.0211 | -0.0616 |
| Time to cross both blinders (ms) | 396 | 326 |

impedance to traverse both blinders does not exceed the time delay for the pre-determined OOS relay settings. The relay recognized the swing impedance behaviour as a fault and should be handled by other protection schemes and misjudged this as stable swing. This situation causes the OOS relay to mis-operate and hence causing severe damage to the generator. On the contrary, the adaptive OOS protection setting does not miss-operate in this condition as displayed in Fig. 9(b). The result demonstrates that the swing impedance traverses both blinder elements of the relay in 348 ms which exceed the time delay of 326 ms set for the relay. This outcome implies that the adaptive relay setting recognized the changes in the system operating condition and adapted its settings to suit to the current operating condition that resulted in the appropriate trip decision to mitigate the impact of the disturbance in the system.

### C. Case C

During power system operations, it is possible for a recoverable stable swing to enter the relay characteristic following a fault in the system. A stable swing is determined as recoverable if the rotor angle separation between two or more group of generators is less than 120° [34]. The case discussed in this subsection investigates the performance of the OOS relay in an unusual operating condition, where impedance swing corresponding to a recoverable stable swing enter the OOS relay characteristic causing the relay to mal-operate. In this case, a three-phase fault cleared 566 ms after the fault inception is considered as the disturbance in the system. It is assumed all three generators are online. Therefore, there is a 50% increase of the inertia constant and a 50% decrease of the combined transient reactance in Generator #10 seen by the OOS relay element. In addition, the generator is assumed to operate at 50% of its internal voltage under normal operating condition. Although this condition is not a widespread problem, protection engineers have reported that this possibility exists for some types of automatic voltage regulators [35]. Similarly, with other cases discussed in this paper, the performance of the OOS relay at Generator #10 is analysed. Fig. 10 exhibits the generator rotor angle in the system following the disturbance. The figure demonstrates that Generator #10 maintains its synchronism with the rest of the system following the disturbance. The rotor angle responses of all the generators indicate that the system is likely to recover from the disturbance because the rotor angle separation between Generator #10 and the rest of the system does not exceed 120°. Consequently, an OOS relay scheme applied at a generator must not operate for recoverable swings because losing a generator due to relay maloperation may turn a recoverable event into a major system outage [34]. Although the system maintains its

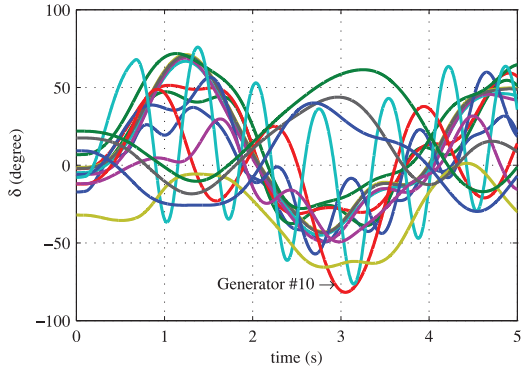


Fig. 10. Rotor angle for all generator for Case C.

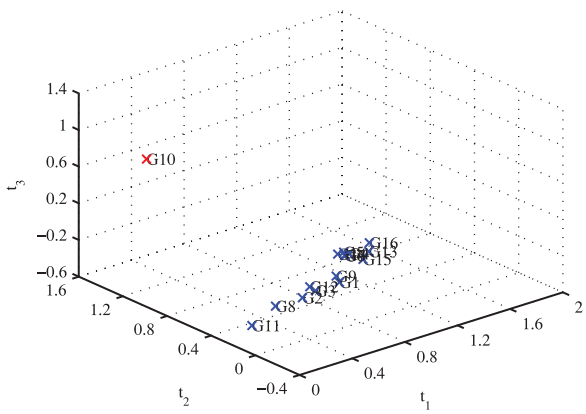


Fig. 11. Coherency plot for Case C.

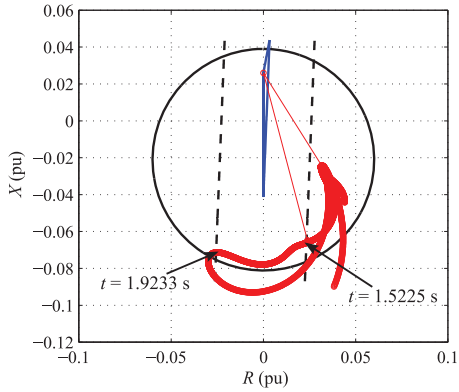


(a)

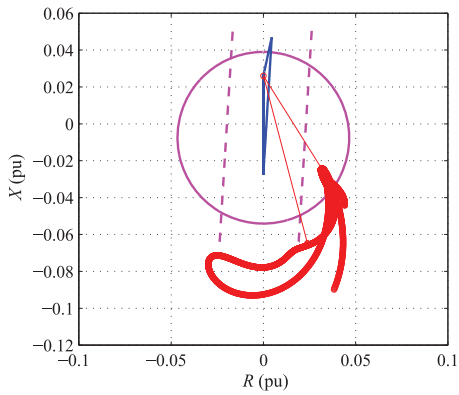


(b)

Fig. 12. Relay settings for Case C (a) Pre-determined (b) Adaptive.

synchronism following the disturbance, not all generators are oscillating in unison. Fig. 11 shows the coherency plot using the ICA method [14]. The figure shows that Generator #10 oscillates against the other generators even though the whole system is still maintains its synchronism. The purpose of coherency identification technique is to identify the coherent groups of generators by analysing the signals from the system when it is difficult to these coherent groups by using visual inspection of the signals [36]. Fig. 12 represents the swing impedance trajectories for two different OOS relay settings. The OOS protection settings in Fig. 12(a) signify the pre-determined OOS relay settings calculated during relay commissioning. In contrast, the adaptive OOS relay settings displayed in Fig. 12(b) are calculated based on the current operating condition of Generator #10. Table IV summarises the pre-determined and adaptive settings of the OOS relay used in this exercise. It is observed from Fig. 12(a) that the swing impedance crosses both blinder elements of relay settings in 401 ms. This indicates that the time for the swing impedance to traverse both blinders exceeds the time delay of 396 ms set in the pre-determined OOS relay settings. Therefore, the relay recognizes the swing impedance behaviour as an OOS condition and initiates a trip signal to isolate Generator #10 from the system. However, it has been discussed earlier that the system is recoverable, following the disturbance considered in this study. Therefore, the OOS relays at Generator #10 must not operate under this condition because it will exacerbate the impact of disturbance to the system [34].

TABLE IV
OOS RELAY SETTINGS FOR CASE C

| Types of setting | Pre-determined | Adaptive |
|---|---|---|
| $d$ (pu) | 0.0244 | 0.0205 |
| $D_{mho}$ (pu) | 0.1201 | 0.0931 |
| $C_{mho}$ (pu) | -0.0211 | -0.0075 |
| Time to cross both blinders (ms) | 396 | 382 |

On the contrary, the impedance trajectory displayed in Fig. 12, which are calculated using the adaptive OOS protection scheme proposed in this paper, does not mal-operate in this condition. The result shows that the swing impedance trajectory did not traverse across the supervisory blinding zone of the relay. Therefore, the adaptive settings of the OOS relay do not initiate a trip signal to isolate the generator from the system. The result implies that the proposed method adapts its settings to suit the current operating situation, which provides appropriate protection and control actions that prevents relay maloperation. Therefore, by ensuring appropriate protection action for the system, the proposed adaptive OOS protection system prevents a false trip of a generator that is caused by relay maloperation.

False tripping of a generator during a stressed operating condition may increase the stress level in other parts of the system. This may trigger cascading tripping event of various protections

in the network. Consequently, cascading events occurring in the network increase the level of stress to the system and eventually cause the catastrophic wide-area blackout. The blackout report published by IEEE Power and Energy Society [1] corroborated this fact. Therefore, reducing the likelihood of generator OOS relay maloperation reduces the likelihood of wide-area blackout in the system.

## VII. Conclusion

An adaptive OOS protection for generators in a power system has been proposed. The approach is based on the EEAC method to determine the CCA and CCT of the system. This calculation is crucial in determining the setting of an OOS protection system. To ensure the relay setting adapts with the current operating condition, the coherent groups of generators are identified using the ICA technique reported in [14] and the dynamic model parameters of the system are estimated using UKF approach proposed in [15]. The coherent groups of generators in the system are identified in near real time and the dynamic model parameters in the system are estimated recursively to obtain an accurate and dynamic model representation of the system. Consequently, the setting of OOS protection is recalculated based on the estimated dynamic models reflecting the existing power system operation. The dependability and security are validated by comparing the outcome of the relay with the response of the rotor angle in the system. The changes in the generator operating condition in the system have significant impact on the effectiveness of OOS relay operation for generator protection. Nevertheless, the method proposed in this paper accurately detects the OOS condition even with the changes in system operating conditions.

## References


[1] P. Kundur, C. Taylor, and P. Pourbeik, "Blackout experiences and lessons, best practices for system dynamic performance, and the role of new technologies," *IEEE Power Eng. Soc. Special Publ.*, 2007, 07TP190.

[2] A. Abdelaziz, M. Irving, M. Mansour, A. El-Arabaty, and A. Nosseir, "Adaptive protection strategies for detecting power system out-of-step conditions using neural networks," *Proc. Inst. Elect. Eng., Gen., Transm. Distrib.*, vol. 145, pp. 387–394, Jul. 1998.

[3] V. Centeno, A. Phadke, A. Edris, J. Benton, M. Gaudi, and G. Michel, "An adaptive out-of-step relay [for power system protection]," *IEEE Trans. Power Del.*, vol. 12, no. 1, pp. 61–71, Jan. 1997.

[4] S. Paudyal, G. Ramakrishna, and M. Sachdev, "Application of equal area criterion conditions in the time domain for out-of-step protection," *IEEE Trans. Power Del.*, vol. 25, no. 2, pp. 600–609, Apr. 2010.

[5] B. Shrestha, R. Gokaraju, and M. Sachdev, "Out-of-step protection using state-plane trajectories analysis," *IEEE Trans. Power Del.*, vol. 28, no. 2, pp. 1083–1093, Apr. 2013.

[6] K. So, J. Heo, C. Kim, R. Aggarwal, and K. Song, "Out-of-step detection algorithm using frequency deviation of voltage," *IET Gen., Transm. Distrib.*, vol. 1, pp. 119–126, Jan. 2007.

[7] P. Kundur, *Power System Stability and Control*. New York, USA: McGraw-Hill, 1994.

[8] A. G. Phadke and J. S. Thorp, *Computer Relaying for Power Systems*. Hoboken, NJ, USA: Wiley, 2009.

[9] E. Bernabeu, J. Thorp, and V. Centeno, "Methodology for a security/dependability adaptive protection scheme based on data mining," *IEEE Trans. Power Del.*, vol. 27, no. 1, pp. 104–111, Jan. 2012.

[10] I. Abdulhadi, "Facilitating the validation of adaptive power system protection through formal scheme modelling and performance verification," Ph.D. dissertation, Univ. Strathclyde, Glasgow, U.K., Aug. 2013.

[11] C. Mozina and J. Gardell, "IEEE tutorial on the protection of synchronous generators (second edition)," *IEEE Power Eng. Soc. Special Publ. IEEE Power Syst. Relay. Committee*, 2011.

[12] *IEEE Guide for AC Generator Protection*, IEEE Standard C37.102-2006 (Revison of IEEE Standard C37.102-1995), Feb. 2007, pp. 1–177.

[13] Y. Xue, T. Van Custem, and M. Ribbens-Pavella, "Extended equal area criterion justifications, generalizations, applications," *IEEE Trans. Power Syst.*, vol. 4, no. 1, pp. 44–52, Feb. 1989.

[14] M. Ariff and B. Pal, "Coherency identification in interconnected power system—An independent component analysis approach," *IEEE Trans. Power Syst.*, vol. 28, no. 2, pp. 1747–1755, May 2013.

[15] M. Ariff, B. Pal, and A. Singh, "Estimating dynamic model parameters for adaptive protection and control in power system," *IEEE Trans. Power Syst.*, vol. 30, no. 1, pp. 829–839, Mar. 2015.

[16] *IEEE Guide for Synchronization, Calibration, Testing, and Installation of Phasor Measurement Units (PMUs) for Power System Protection and Control*, IEEE Standard C37.242-2013, Mar. 2013.

[17] P. M. Anderson, *Power System Protection*. New York, USA: McGraw-Hill, 1999.

[18] Y. Zhang, L. Wehenkel, P. Rousseaux, and M. Pavella, "SIME: A hybrid approach to fast transient stability assessment and contingency selection," *Int. J. Elect. Power Energy Syst.*, vol. 19, pp. 195–208, Mar. 1997.

[19] R. Treinen, V. Vittal, and W. Kliemann, "An improved technique to determine the controlling unstable equilibrium point in a power system," *IEEE Trans. Circuits Syst. I, Fundam. Theory Appl.*, vol. 43, no. 4, pp. 313–323, Apr. 1996.

[20] H.-D. Chiang, F. Wu, and P. Varaiya, "Foundations of the potential energy boundary surface method for power system transient stability analysis," *IEEE Trans. Circuits Syst.*, vol. 35, no. 6, pp. 712–728, Jun. 1988.

[21] H.-D. Chiang and J. Thorp, "The closest unstable equilibrium point method for power system dynamic security assessment," *IEEE Trans. Circuits Syst.*, vol. 36, no. 9, pp. 1187–1200, Sep. 1989.

[22] H.-D. Chiang, F. Wu, and P. Varaiya, "A BCU method for direct analysis of power system transient stability," *IEEE Trans. Power Syst.*, vol. 9, no. 3, pp. 1194–1208, Aug. 1994.

[23] V. Vittal, P. Sauer, S. Meliopoulos, and G. Stefopoulos, "Online transient stability assessment scoping study" Ithaca, NY, USA, Rep. no. 05-04, 2005, Power Systems Engineering Research Center (PSERC) Project Report.

[24] A. Hyvärinen and E. Oja, "A fast fixed-point algorithm for independent component analysis," *Neural Comput.*, vol. 9, pp. 1483–1492, Oct. 1997.

[25] S. Julier and J. Uhlmann, "Unscented filtering and nonlinear estimation," *Proc. IEEE*, vol. 92, no. 3, pp. 401–422, Mar. 2004.

[26] P. Kundur *et al.*, "Definition and classification of power system stability IEEE/CIGRE joint task force on stability terms and definitions," *IEEE Trans. Power Syst.*, vol. 19, no. 3, pp. 1387–1401, Aug. 2004.

[27] K. Anaparthi, B. Chaudhuri, N. Thornhill, and B. Pal, "Coherency identification in power systems through principal component analysis," *IEEE Trans. Power Syst.*, vol. 20, no. 3, pp. 1658–1660, Aug. 2005.

[28] J. Thambirajah, N. Thornhill, and B. Pal, "A multivariate approach towards interarea oscillation damping estimation under ambient conditions via independent component analysis and random decrement," *IEEE Trans. Power Syst.*, vol. 26, no. 1, pp. 315–322, Feb. 2011.

[29] A. G. Phadke and J. S. Thorp, *Synchronized Phasor Measurements and Their Applications*. New York, USA: Springer-Verlag, 2008.

[30] G. Ziegler, *Numerical Distance Protection: Principles and Applications*. Hoboken, NJ, USA: Wiley, 2011.

[31] G. Rogers, *Power System Oscillations*. Norwell, MA, USA: Kluwer, 2000.

[32] B. C. Pal and B. Chaudhuri, *Robust Control in Power Systems*. New York, USA: Springer, 2005.

[33] C. Mozina and J. Gardell, "IEEE tutorial on the protection of synchronous generators," *IEEE Power Eng. Soc. Special Publ. IEEE Power Syst. Relay. Committee*, 1995.

[34] D. Reimert, *Protective Relaying for Power Generation Systems*. Boca Raton, FL, USA: CRC, 2006.

[35] J. Berdy, "Out-of-step protection for generators," in *Proc. Georgia Inst. Technol. Protect. Relay Conf.*, May 1976, pp. 1–26.

[36] N. Senroy, "Generator coherency using the Hilbert-Huang transform," *IEEE Trans. Power Syst.*, vol. 23, no. 4, pp. 1701–1708, Nov. 2008.

**M. A. M. Ariff** (S'12–M'15) received the B.Eng. degree in electrical engineering (Hons.) and the M.Eng degree in electrical power from Universiti Teknologi Malaysia (UTM), in 2008 and 2010, respectively, and the Ph.D. degree from Imperial College London, London, U.K., in 2014.

Currently, he is a Senior Lecturer with Universiti Tun Hussein Onn Malaysia (UTHM), Batu Pahat Johor, Malaysia. His current research interests include power system dynamics, coherency identification, adaptive protection in power system, and controlled separation for blackout prevention.

**B. C. Pal** (M'00–SM'02–F'13) received the B.E.E. (Hons.) degree in electrical engineering from Jadavpur University, Calcutta, India, in 1990, the M.E. degree in electrical engineering from the Indian Institute of Science, Bangalore, India, in 1992, and the Ph.D. degree in electrical engineering from Imperial College London, London, U.K., in 1999.

Currently, he is a Professor of Power Systems in the Department of Electrical and Electronic Engineering, Imperial College London. His current research interests include state estimation, and power system dynamics..